

SEASONAL STRUCTURAL CHANGES OF PHLOEM CELLS IN *GINKGO BILOBA* L.SHAN LI^{1,2,3}, XIN LI⁴, YAFANG YIN^{1,2}, XIAOMEI JIANG^{1,2}, JINGMING ZHENG⁴,
LI WANG⁵, ZHICHENG CHEN⁶ AND PETER PRISLAN^{7*}¹Department of Wood Anatomy and Utilization, Research Institute of Wood Industry, Chinese Academy of Forestry, Beijing 100091, P.R. China²Wood Collections (WOODPEDIA), Chinese Academy of Forestry, Beijing 100091, P.R. China³School of Environmental Science and Engineering, Shaanxi University of Science & Technology, Xi'an, 710021, P.R. China⁴College of Forestry, Beijing Forestry University, Beijing, 100083, P.R. China⁵Center for Biological Imaging, Institute of Biophysics, Chinese Academy of Science, Beijing, 100101, P.R. China⁶Research Institute of Forestry New Technology, Chinese Academy of Forestry, Beijing 100091, China⁷Slovenian Forestry Institute, Večna pot 2, SI-1000 Ljubljana, Slovenia*Corresponding author's email: peter.prislan@gozdis.si

Abstract

Ginkgo biloba is a non-coniferous gymnosperm tree species growing in China and widely cultivated as ornamental tree. Exploring seasonal structural changes in phloem cells of *Ginkgo biloba* could provide better understanding of the relationship between phloem structure and function. Stems of *Ginkgo biloba* saplings were sampled at regular intervals during different seasons and then prepared for observation with light microscopy and transmission electron microscopy. Light microscopy was used for identification of non-conducting and conducting phloem and for histometric comparison between sampling dates. Ultrastructure (cell organelle presence and distribution) of phloem sieve cells and parenchyma was observed to better understand seasonal changes in phloem cells. Our results showed that most early phloem sieve cells collapsed at the end of the growing season, while most late phloem sieve cells did not collapse till the next spring. Sieve cells in the youngest phloem were characterized by square shape with larger radial diameter and slightly thicker cell walls compared to cambial cells. Their lumina were mostly empty, although some organelles (endoplasmic reticulum, plastids) could be found close to the cell walls. In the older (nonconducting) phloem the shape of sieve cells became partly collapsed with completely empty lumina. Furthermore, pores are mostly open and callose was not present on sieve plates neither in the youngest nor in the older phloem. Most phloem parenchyma cells contain large vacuoles, lipid droplets and amyloplasts, with those in the youngest phloem showing evident seasonal changes, i.e., the cytoplasm was denser in spring and winter compared to summer and autumn, and lipid droplets appeared to be at the highest density/frequency in winter compared with other seasons. In conclusion, phloem sieve cells of *G. biloba* undergo obvious seasonal structural changes depending on their ages, which is also in accordance with their seasonal conducting functions in these deciduous trees. Youngest phloem parenchyma cells also showed seasonal structural variation with regards to cytoplasm density and frequency of lipid droplets.

Key words: *Ginkgo biloba*, Phloem, Parenchyma, Ultrastructure, Seasonal changes, Sieve cells.

Introduction

Phloem functions as the main tissue is responsible allocating photosynthetic assimilates and storage, transporting macromolecules such as phenolics and volatile organic compounds, as well as defending against external threats (Bel, 2003; Keeling & Bohlmann, 2006; Turgeon & Wolf, 2009). Phloem in gymnosperms consists of sieve cells, Strasburger cells as well as axial and ray parenchyma cells. Sieve cells are characterized by sieve areas on lateral and end walls and are responsible for the long-distance transport of solutes (Evert, 2006; Holbrook & Knoblauch, 2018). The anatomical characteristics of phloem are crucial for understanding its transport capacity (Ronellenfitsch *et al.*, 2015) and its response to changing environmental conditions (Dannoura *et al.*, 2018; Gričar *et al.*, 2018; Hesse *et al.*, 2018; Salmon *et al.*, 2019). Seasonal structural changes of phloem might provide useful information to understand its physiological and biological function (Hao & Wu, 1992; Prislan *et al.*, 2018).

Ginkgo biloba is a non-coniferous gymnosperm tree species growing in China and widely cultivated as ornamental tree throughout the world (Qie & Wang, 2011). Studies on seasonal phloem formation are crucial to get a comprehensive understanding about radial growth in *G. biloba*. While its microscopic structure and phenology of phloem have been reported by den Outer (1967) and Wang (2014), seasonal observations of ultrastructural changes in phloem cells in *G. biloba* are rare.

Phloem tissue in general can be divided into conducting and nonconducting phloem. Conducting phloem is mainly responsible for conducting photosynthetic assimilates, while storage is the main function of nonconducting phloem (Angyalossy *et al.*, 2016). In *G. biloba*, the conducting phloem can be distinguished from the nonconducting phloem based on the shape and dimensions of cells; sieve cells in conducting phloem have a more or less square shape in cross section, while the axial parenchyma cells have a rounded shape and contain cytoplasm. Typically, sieve cells are connected through plasmodesmata with Strasburger cells, and both cell types have distinctive

ultrastructural characteristics (Oparka & Robert, 1999). Conduction of photosynthetic assimilates takes place in sieve cells of the youngest conducting phloem which accounts for a small proportion of the phloem tissue. Nonconductive sieve cells are either covered with callose in their sieve areas, or entirely free of this substance (Evert, 2006). Nevertheless, it is unknown how callose distribution varies among different seasons in *G. biloba* phloem. Moreover, most conifers show sieve cells that cease to function in the current year, while temperate ring-porous hardwood species show sieve elements that can remain functional for longer than 10 years (Holdheide, 1951). These sieve elements show a seasonal pattern of dormancy and reactivation seasonally, with auxin playing a potentially important role (Aloni & Peterson, 1997). It is unknown how sieve cells in *G. biloba* change seasonally especially from ultrastructural level.

In most temperate species, phloem growth rings can be clearly distinguished in the youngest phloem increment based on differences in morphological features of early and late phloem cells, as well as the presence of a tangential band of axial parenchyma cells (Gričar *et al.*, 2016). Besides, in the nonconducting phloem, the sieve cells are more flattened and are not conductive anymore (Evert, 2006). Furthermore, age-related secondary changes can be observed, such as inflation of axial parenchyma cells and development of sclereids (Esau, 1969; Evert, 2006). However, according to den Outer (1967) phloem growth rings in *Ginkgo biloba* are indistinct, composed of bands of 1~3 layers of sieve cells alternate with bands of 1~2 parenchyma cells.

In recent years, the number of studies on phloem anatomy have increased (Jyske & Teemu, 2014; Steppe *et al.*, 2015; Suuronen & Pranovich, 2015; Angyalossi *et al.*, 2016), as well as phloem transport mechanism (Hölttä *et al.*, 2009; Holbrook & Knoblauch, 2018; Rockwell *et al.*, 2018; Schepper *et al.*, 2013). Detailed investigation of phloem seasonal changes especially in ultrastructural level would be helpful for understanding their biological functions. In this study, seasonal ultrastructural changes of phloem (including conducting or nonconducting phloem cells) of *G. biloba* were observed. The goals of the study were: 1) to evaluate the timing of annual phloem formation; 2) to directly compare the ultrastructural differences of phloem cells (mainly sieve cells, phloem axial parenchyma cells, and phloem ray parenchyma cells) of *G. biloba* during different seasons.

Materials and Methods

Samples were collected from four healthy, 5-6 years old *G. biloba* seedlings, with plant height of 90-100 cm, in different season; i.e., in summer (June 15th 2018), autumn (September 15th 2018), winter (December 15th 2018) and spring (March 15th 2019). These saplings were previously sown in Beijing Institute of Landscape Architecture, transferred to 10-L pots with organic soil in spring of 2018. All seedlings were irrigated regularly and maintained healthy. In April of 2018, these saplings were transported to a glasshouse in the Chinese

Academy of Forestry and allowed adaption in the microenvironment for about one month before the sampling started. During the whole sampling period, all seedlings were well-watered.

In each season one individual seedling was selected for sampling and observation. Sample blocks (1 mm*1 mm*2 mm) were collected from the middle part of the main stems (around 1.5 cm in diameter at the sampling position) of the seedlings and cut under water with fresh razor blades. Each sample included phloem, cambium and two to three youngest xylem growth rings. Immediately after sampling, the blocks were stored in a fixative (2.5% glutaraldehyde, 0.1 M phosphate buffer, pH 7.3) at 4°C for different numbers of days due to labor shortage before post-fixation. Subsequently, the samples were washed in 0.1 M phosphate buffer, rinsed and post-fixed with 2% buffered osmium tetroxide for 2 hours. Following that, the samples were dehydrated in a series of ethanol concentrations (30%, 50%, 70%, 90%) and embedded in Epoxy resin (SPI, Westchester, USA) at 60°C.

Transversal and radial semi-thin sections (about 200 nm thick) and ultrathin sections (about 70 nm thick) were cut from the embedded samples with an ultramicrotome (Leica EM UC6, Leica Microscopy Imaging System, Buffalo Grove, USA). Semi-thin sections were stained with 1% toluidine blue, and ultrathin sections were double-stained with uranyl acetate and lead citrate. Semi-thin sections were photographed using a light microscope (Olympus BX 50, Olympus Corporation, Tokyo, Japan), and ultrathin sections were photographed using a transmission electron microscope, i.e., TEM (Tecnai Spirit, FEI company, Hillsboro, USA). ImageJ software (National Institutes of Health, Bethesda, Maryland, USA) was used to evaluate morphological features of sieve cells and parenchyma cells from semi-thin sections.

In this paper, we distinguish early and late phloem growth rings of *G. biloba*; Early phloem growth rings consist of only sieve cells arranging in radial rows with scattering phloem parenchyma cells, while late phloem growth rings start from a radial band of phloem axial parenchyma cells and consist of alternating layers of sieve cells and axial parenchyma cells. Sieve cells were distinguished by almost empty cellular contents (in some cases only with remaining of cytoplasm), while parenchyma cells were distinguished by complete cytoplasm and abundant cellular organelles. Tangential and radial length of sieve cells and parenchyma cells was measured from transversal semi-thin sections, and axial length of sieve cells and parenchyma cells was measured from longitudinal semi-thin sections (shown in Fig. 1). Minimum 50 cells from younger phloem (3~15 layers of phloem cells from cambium) in each sample per season were measured. Proportions of phloem parenchyma cells were calculated from transversal semi-thin sections for each season, dividing total area of all phloem parenchyma cells by the total area of the measured phloem area, with at least 100 parenchyma cells measured in each sample.

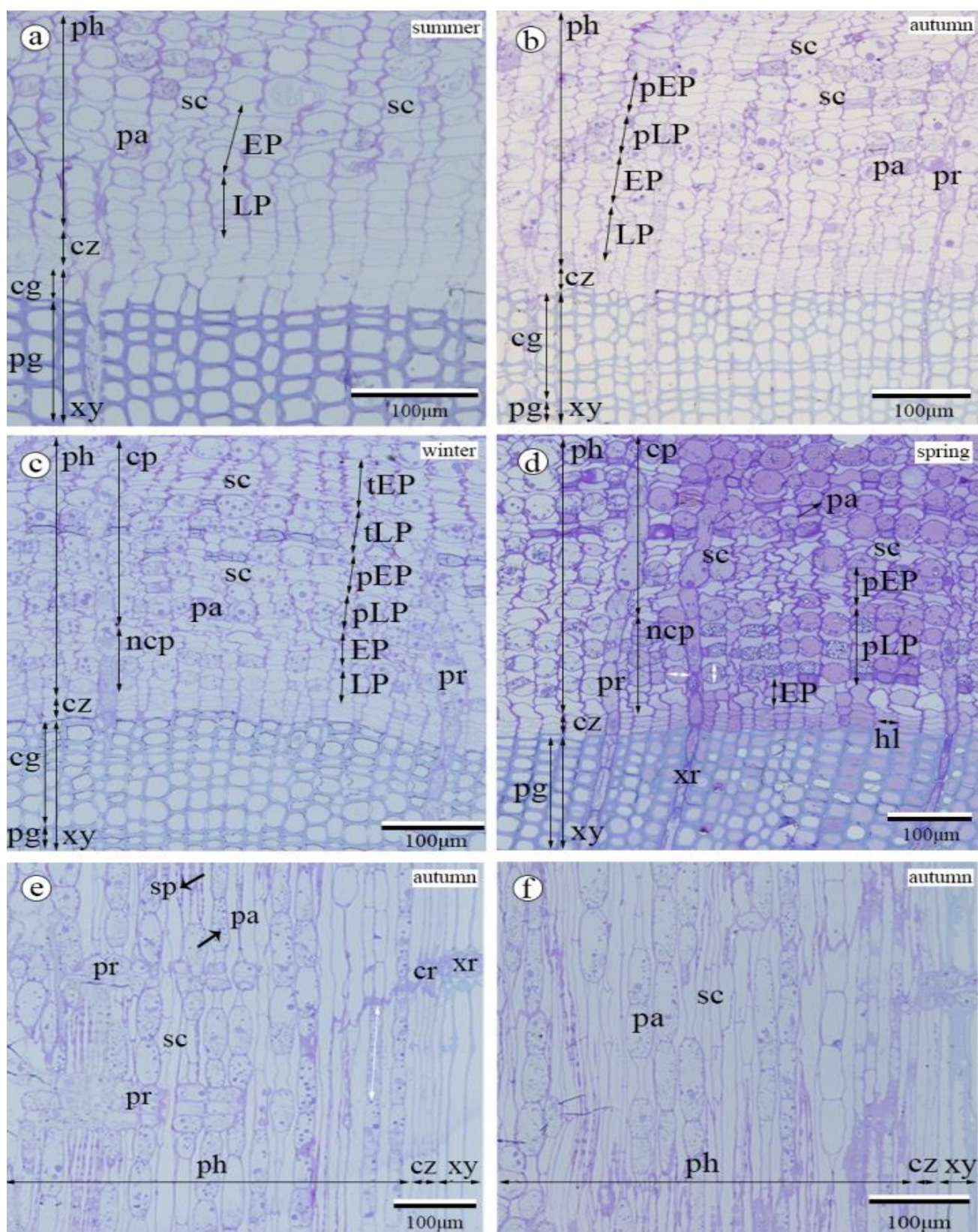


Fig. 1. Seasonal changes of the microscopic characteristics of phloem and xylem in *Ginkgo biloba*. Figure a-d show transversal sections in summer, autumn, winter and spring, with samples collected on June 15th, 2018, September 15th, 2018, December 15th, 2018 and March 15th, 2019, respectively. Figure e-f show longitudinal sections in autumn. Abbreviations are as follows: cg. current year growth ring, cp. conducting phloem, cr. cambial ray cells, cz. cambium zone, EP. early phloem of current growing season, LP. late phloem of current growing season, np. non-conducting phloem, pa. phloem axial parenchyma, pEP. early phloem formed in the previous year, tEP. third-year early phloem, tLP. third-year late phloem, ph. phloem, pg. previous year growth ring, pLP. late phloem formed in the previous year. pr. phloem ray parenchyma cells, pg. previous year growth ring, sc. sieve cell, sp. sieve pore, xr. xylem ray parenchyma cell, xy. xylem. White arrow is the illustration of measurements on axial diameter, radial diameter and axial height of phloem parenchyma cells.

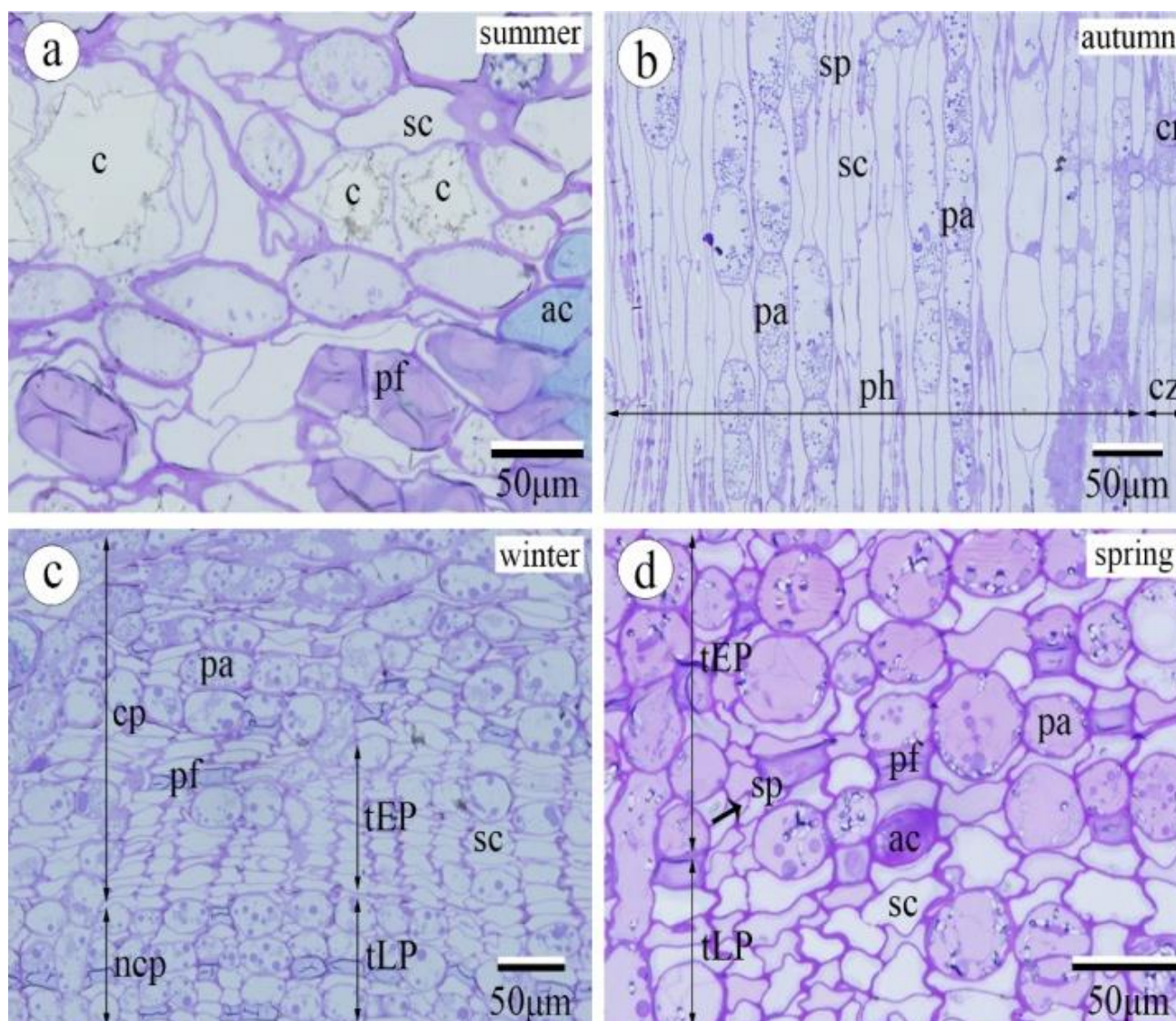


Fig. 2. Structure of cambium and phloem in *G. biloba* under light microscope. Figure a, c-d are transversal sections of phloem and figure b is from longitudinal section showing cambium and phloem. Figures a-b and d show older collapsed phloem tissue. Figure 2a and 2d are images at higher magnification of the third-year phloem growth ring in Figure 1a and 1d, respectively. Abbreviations: ac. albuminous cells, c. crystal, cp. conducting phloem, cr. cambial ray cells, cz. cambium zone, EP. early phloem, LP. late phloem, tEP, third-year early phloem, tLP, third-year late phloem, np. non-conducting phloem, pa. phloem axial parenchyma cell, pf, phloem fiber, ph. phloem, sc. sieve cell, sp. sieve pore.

Results

Microscopic characteristics of phloem and its seasonal variation:

The phloem of *Ginkgo biloba* is mainly composed of axially elongated sieve cells and parenchyma cells as shown from both transversal and radial sections (Fig. 1). The average tangential diameter, radial diameter and axial length of sieve cells of the younger phloem (3~15 layers of phloem cells from cambium) are about $24 \pm 2 \mu\text{m}$, $8 \pm 1 \mu\text{m}$ and $135 \pm 8 \mu\text{m}$, respectively. Sieve cells in the youngest phloem were characterized by square shape with larger radial diameters and slightly thicker cell walls compared to cambial cells. Phloem axial parenchyma cells are arranged in tangential bands, with average tangential diameter around $25 \pm 2 \mu\text{m}$, radial diameter around $15 \pm 2 \mu\text{m}$ and axial length $60 \pm 2 \mu\text{m}$ in the younger phloem. The proportion of phloem parenchyma cells (including axial parenchyma cells and

ray parenchyma cells) in the whole phloem tissue ranged from 20% to 49% in different seasons, with 49% in winter and 20% in summer. Compared with xylem ray cells, the volume of all phloem ray cells enlarged significantly in the older phloem tissue due to secondary changes (i.e. expansion of parenchyma cells) (Fig. 1), and crystals were also more frequent in phloem axial parenchyma cells of the nonconducting phloem (Fig. 2b). Also, the sizes of phloem axial parenchyma cells as well as its cell wall thickness tended to increase due to secondary changes in phloem (Figs. 1, 2). The lipid droplet density/frequency in phloem parenchyma cells of the winter samples was significantly higher than other seasons under light microscopy (Fig. 1a-1d). Newly differentiated xylem cells were observed during the growing season (summer sampling). The width of youngest xylem growth ring was $41 \pm 7 \mu\text{m}$, $117 \pm 8 \mu\text{m}$ and $132 \pm 9 \mu\text{m}$ in summer, autumn and winter time respectively.

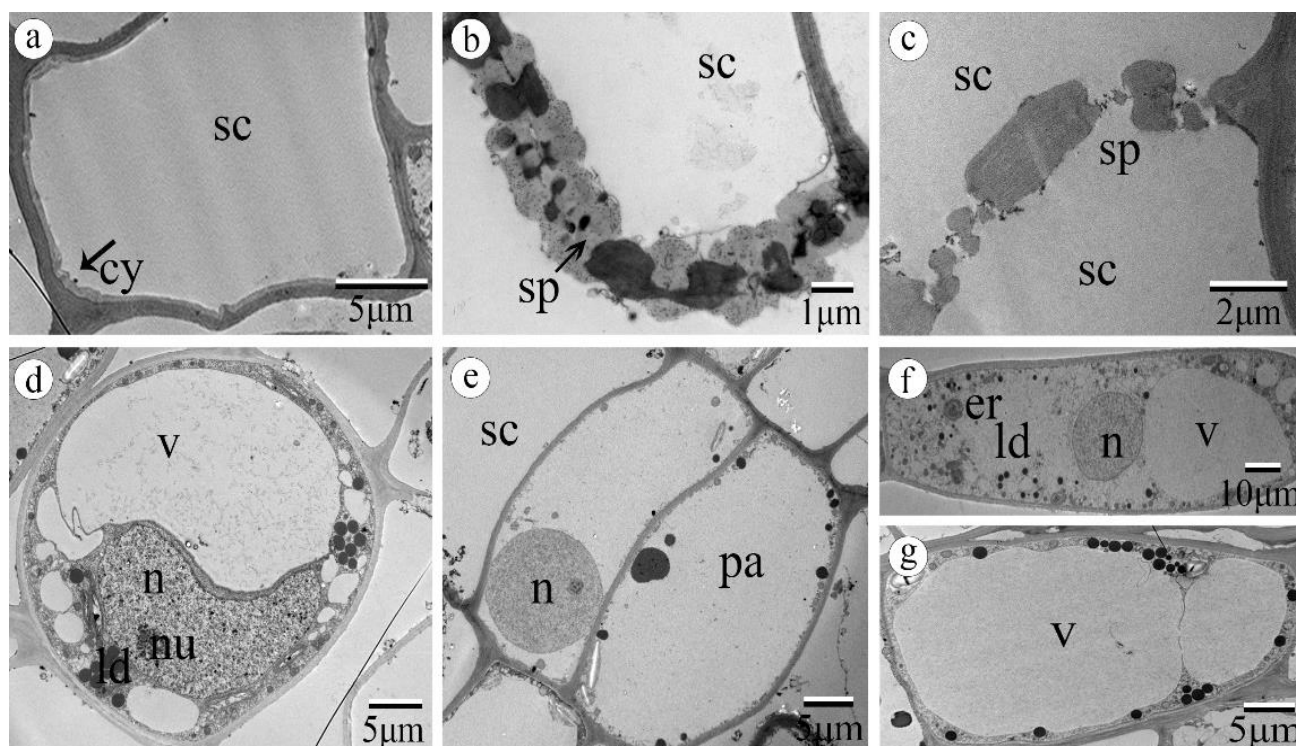


Fig. 3. Ultrastructural characteristics *G. biloba* phloem in summer (June 15th, 2018). (a) Phloem sieve cell in the youngest phloem growth ring (3 cell layers away from cambium) are characterized with thin layer of cytoplasm attached to the cell wall. (b) in the youngest phloem, sieve pores were occluded by the remaining of the cytoplasm. (c) Sieve pores located in old phloem growth ring (14 cell layers away from cambium). (d and f) Axial parenchyma cells located in youngest phloem (3 cell layers away from cambium). (e) Amyloplasts in phloem axial parenchyma cells 5 cell layers away from cambium. (g) Ray parenchyma cell in youngest phloem. Figure f is from longitudinal view and the rest are from transversal view. Abbreviations: cy. cytoplasm, er. endoplasmic reticulum, ld. lipid droplet, mi. mitochondria, n. nucleus, nu. nucleolus, pl. plastid, s. starch, sp. sieve plate, sc. sieve cell, v. vacuole.

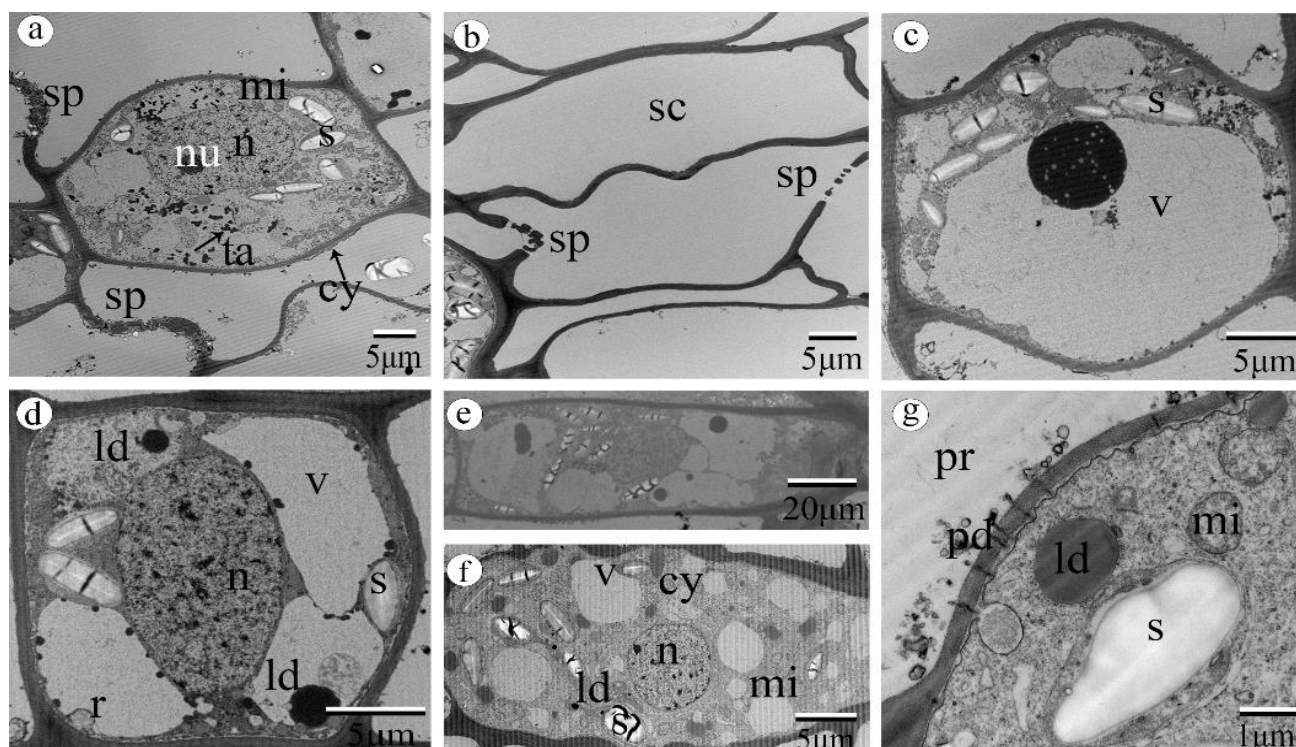


Fig. 4. Ultrastructural characteristics of phloem of *G. biloba* in autumn (September 15th, 2018). (a, c-e) Phloem axial parenchyma cells located in youngest phloem, i.e., 3-4 cell layers away from cambium, (b) Collapsed sieve cells in older phloem, (f, g) Ray parenchyma cells crossing cambium zone to the phloem, with plasmodesmata between ray parenchyma cells clearly visible. Figure e is from longitudinal view and the rest are from transversal view. Abbreviations: cy. cytoplasm, ld. lipid droplet, mi. mitochondria, n. nucleus, nu. nucleolus, pd. plasmodesmata, pr. parenchyma cells, r. rim, s. starch, sc. sieve cell, sp. sieve pore, ta. tannin, v. vacuole.

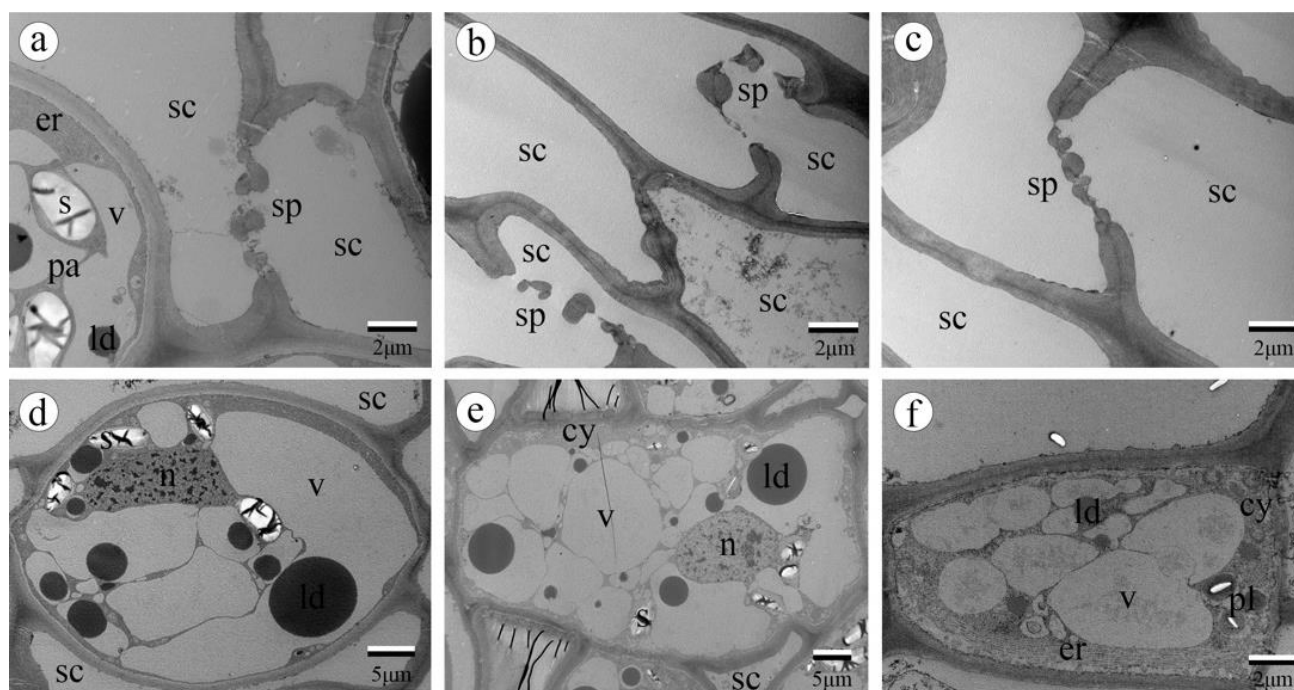


Fig. 5. Ultrastructural characteristics of phloem from transversal sections of *G. biloba* in winter (December 15th, 2018). (a) Sieve pores located in young phloem growth ring (11 cell layers away from cambium) with remaining's of cytoplasm. (b) Sieve cells located in old phloem growth ring showing open sieve pores (about 30 cell layers away from cambium). (c) Sieve cells located in old phloem growth ring showing partly blocked sieve pores (about 34 cell layers away from cambium). (d) Phloem axial parenchyma cells in previous year phloem. (e) Phloem ray parenchyma cells. (f) Newly formed phloem axial parenchyma cells (1 cell layers away from cambium). Abbreviations: cy, cytoplasm, er, endoplasmic reticulum, ld, lipid droplet, n, nucleus, pl, plastid, s, starch, sc, sieve cell, sp, sieve pore, v, vacuole.

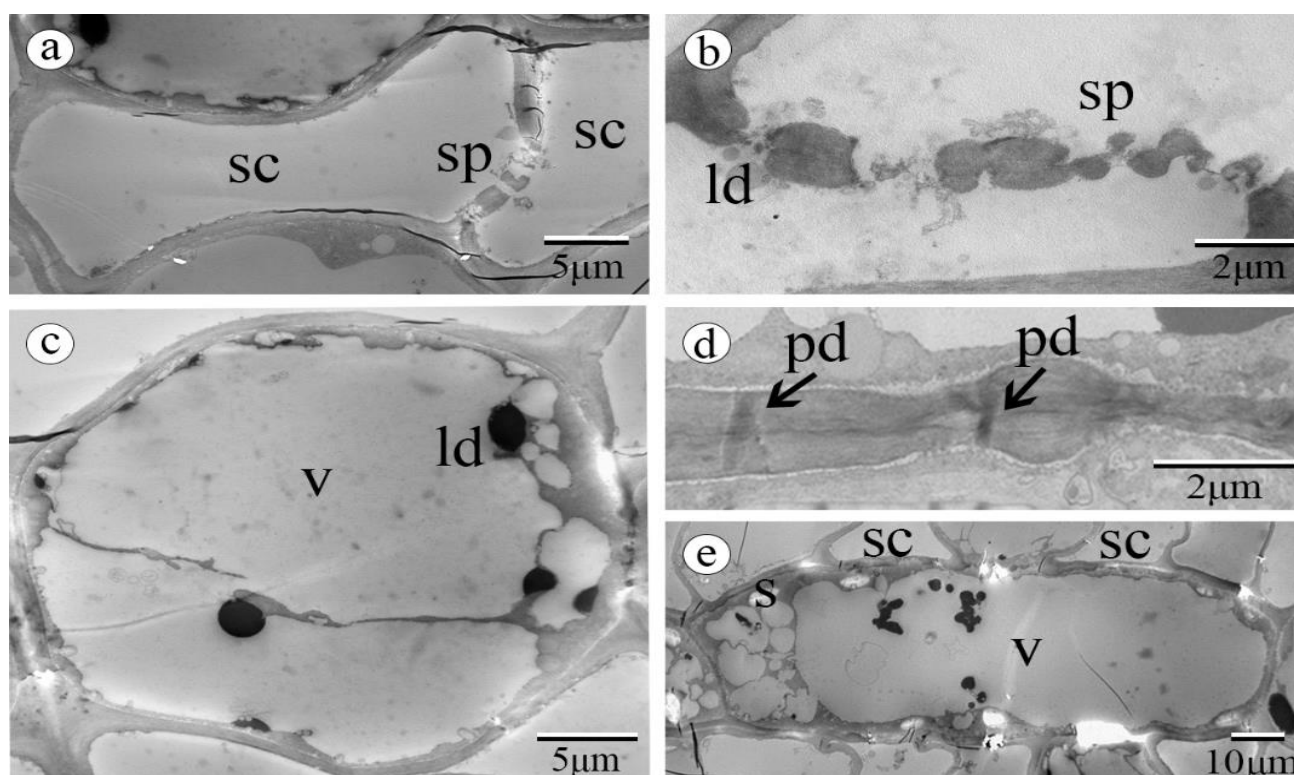


Fig. 6. Ultrastructural characteristics of transversal sections of phloem of *G. biloba* in spring (March 15th, 2019). (a) Sieve cells located in the newly developed phloem growth ring (3 cell layers away from cambium), with sieve pores partly blocked by remaining of cytoplasm. (b) Sieve pores located in the phloem growth ring formed in previous growing season (17 cell layers away from cambium), with sieve pores partly blocked by cytoplasm remaining. (c) Axial parenchyma cells in youngest phloem (4 cell layers away from cambium), with large vacuoles and lipid droplets. (d) Plasmodesmata between axial parenchyma cells. (e) Phloem ray cells with large vacuoles. Abbreviations: ld, lipid droplets, pd, plasmodesmata, s, starch, sc, sieve cells, sp, sieve pore, v, vacuole.

The collapse of sieve cells was also more obvious in older phloem closer to the cortex (Fig. 2d). With the increase of phloem age, the shape of sieve cells changed and became squeezed and partly collapsed. The collapse trend of the sieve cells in the current year phloem is (Fig. 1): about 20% collapsed sieve cells were present in the current year early phloem (EP) during the growing season, and there was almost no collapsed sieve cell in the LP. In autumn, an increasing number of collapsed sieve cells were observed in EP compared to those in summer, while there was still almost no collapsed sieve cells in the LP. In winter, there was a large amount of collapsed sieve cells in the EP, but still there were no collapsed sieve cells in the LP. In the next spring, about 97% collapsed sieve cells were present in the previous year early phloem (pEP), while there was only 29% collapsed sieve cells in the previous year late phloem (pLP). In brief, current year early phloem sieve cells did not show obvious collapse until post-growing season time, i.e., in the winter time, while current year late phloem were not collapsed in the whole year. Similarly, previous year early phloem cells were mostly collapsed while previous year late phloem cells remained non-collapsed over the winter time. Along with the collapse of sieve cells, the neighboring phloem parenchyma cells appeared to enlarge in sizes with thicker cell walls.

Seasonal ultrastructural variation of phloem: In the differentiated phloem closest to the cambium in all seasons, ultrastructure of sieve cells was characterized by relatively turgid shapes and mostly open sieve pores. Cytoplasm was partly present in the cell lumina, or distributed around sieve pores (Figs. 3a-3b, 4a, 5a, 6a). Also, in older phloem sieve pores could be either open or partly blocked by cytoplasm remains (5b-5c). Nevertheless, no clear evidence on callose deposition in sieve fields of the whole phloem tissue was observed. The ultrastructure of phloem axial parenchyma cells and phloem ray parenchyma cells was similar between the sampling dates and they were characterized with dense cytoplasm, large and few small vacuoles (Fig. 3d, 4c, 4d-4f, 5d-5f, 6c, 6e). Abundant lipid droplets and vesicles were distributed in the cytoplasm of the phloem axial parenchyma cells (Fig. 4d). Organelles such as nucleus, nucleolus, a large number of mitochondria and amyloplasts, substances such as tannins and lipid droplets were distributed in phloem parenchyma cells (Figs. 3-6). The plasmodesmata between phloem ray parenchyma cells were clearly visible (Fig. 4g, 6d). In contrast, ultrastructure of sieve cells varied in different seasons

Discussion

A distinguishing feature of phloem in *G. biloba* is the abundance of phloem axial parenchyma cells, occupying almost 49% of the total phloem area as observed under the transversal section, which agrees with previous study by den Outer (1967). Many angiosperm tree species have sieve tubes normally surrounded by abundant axial phloem parenchyma cells. In contrast, the phloem of conifers consists mainly of sieve cells, Strasburger cells, relatively less amount of axial and ray

parenchyma cells (Schulz, 1990; Bowes, 1997; Sevanto, 2014, 2019), and specialized polyphenolic parenchyma (PP) cells which defend parasitic and pathogenic organisms in some species (Franceschi *et al.*, 2000; Krekling *et al.*, 2000). While the Strasburger and companion cells die when their partnered conducting elements form callose and lose their protoplast, many ray and axial parenchyma cells remain alive, in some cases for more than 20 years (Spicer, 2014). *G. biloba* has abundant phloem parenchyma cells storing nutrients and water, the large vacuoles distributed in its phloem parenchyma cells are crucial to maintain phloem cell turgor, and numerous plasmodesmata in between phloem axial parenchyma cells ensures efficient nutrients exchange. In nonconducting phloem, some axial parenchyma cells differentiate into sclereids in later developmental stages, as observed from phloem fiber cells of *G. biloba*.

It is generally believed that the width of the conducting phloem is generally narrower than the corresponding increment of xylem (Evert, 2006). During ontogeny, sieve cells undergo a controlled disintegration process known as “programmed cell semi-death” (Esau, 1969), where the larger cellular organelles are degraded and removed, i.e., the nucleus gradually disintegrates, the vacuolar membrane disappears as cytoskeletal elements, ribosomes, Golgi bodies and the mitochondria are reduced. Fully functional sieve cells therefore contain the plasma membrane, a thin layer of parietal cytoplasm, composed of mostly endoplasmic reticulum and mitochondria. Finally, the collapse of the phloem tissue comprises the true death of the sieve cells, with the decrease in turgor, related with the cessation of photoassimilate conduction (Evert, 1990, Van Bel, 2003). Meanwhile, the plasmodesmata between sieve element walls are converted into sieve pores that facilitate flow (Sjölund, 1997). Collapse of sieve cells is part of secondary changes in phloem and is an irreversible process. Evert (2006) reported that phloem sieve cells in branches of adult *G. biloba* were partly collapsed especially in older phloem, while in our study seasonal changes of sieve cell collapse was recorded more in detail. It is interesting that early phloem sieve cells of *G. biloba* were more prone to collapse compared with late phloem sieve cells, which might be genetically controlled and also affected by seasonal physiological activities. The conductive sieve cells from different ages of phloem sieve cells could coordinate with phloem parenchyma cells even after growing season to transport nutrients. In addition, it should be notified that the deciduous phenology of *G. biloba* has major impact on the seasonality in the secondary phloem structure shown in our study.

Studies have shown that substances such as remains of cytoplasm, callose etc. often accumulate around all the sieve pores of phloem in some gymnosperm species, however, they are only distributed in conductive sieve cells in other gymnosperm species including *G. biloba* (Li, 2012), and callose is involved in the differentiation of sieve pores (Nedukha, 2016). We were not able to distinguish callose in our ultrastructural observations, and substances accumulated in the sieve pores of newly

developed sieve cells were regarded as remains of cytoplasm in this species. The growing condition, i.e. the glasshouse might be a potential factor influencing the observed result in our study, such as complete absence of callose. Nevertheless, it is unknown whether the presence of cytoplasmic remains in phloem sieve pores was *in situ* or due to injury during sampling. The appearance of callose reduced efficiency of nutrient transport in phloem (Koh *et al.*, 2012), meanwhile preventing viruses and other external threats (Yao *et al.*, 2012). Some researchers believe that the occlusion of sieve pores by callose indicate important mechanisms of phloem sieve pore formation, displacing cellulose microfibrils in the wall so that large sieve openings could be left behind afterwards. However, others believe that it is produced as a response to mechanical injury during sample collection or as a defense mechanism against pathogens, and disappear when the fixation solution is improved (Anderson & Cronshaw, 1969; Zhao & Hu, 1985). This might apply to the remains of cytoplasm blocking the sieve cells of our study as well, while there is no clear evidence resolving the controversy about the mechanism on its production to our knowledge.

Conclusions

In conclusion, the collapse of phloem sieve cells differed according to the ages, such as early phloem vs late phloem, previous year vs current year and so on. The collapse of sieve cells starts first in early phloem and then gradually continues in late phloem. Early phloem sieve cells in the current year phloem collapsed at end of the growing season, while most late phloem sieve cells were conductive all year around. Similarly, previous year late phloem cells were mostly collapsed while previous year early phloem cells were conductive. The collapse of sieve cells were also more obvious in phloem closer to the bark in the winter time. Our results support previous findings that the collapse of sieve cells is part of secondary changes in phloem and is an irreversible process. In each season, with the increase of phloem age, the proportion of sieve pores blocked by unknown substances (probably the remains of cytoplasm) tends to decrease. Most of the axial parenchyma cells contain large vacuoles, lipid droplets, starch and other substances in different seasons, suggesting that no obvious seasonal ultrastructural changes occur in phloem parenchyma cells.

Acknowledgments

We acknowledge Runmei Zhao, Xiangquan Guo, Xianchong Wan, Jianhua Shu and Hongyan Sun for providing space in greenhouse and rain shelter for the *G. biloba* saplings, as well as the regular maintenance. This work was supported by Beijing Natural Science Foundation (6184048) and National Natural Science Foundation of China (32071691). Anonymous reviewers are also acknowledged for their valuable suggestions.

References

- Aloni, R. and C.A. Peterson. 1997. Auxin promotes dormancy callose removal from the phloem of *Magnolia Kobus* and callose accumulation and earlywood vessel differentiation in *Quercus robur*. *J. Plant. Res.*, 110 (1): 37-44.
- Anderson, R. and J. Cronshaw. 1969. The effects of pressure release on the sieve plate pores of *Nicotiana*. *J. Ultrastruct. Res.*, 29(1-2): 50-59.
- Angyalossy, V., M.R. Pace, R.F. Evert, C.R. Marcati, A.A. Oskolski, T. Terrazas, E. Kotina, F. Lens, S.C. Mazzoni-Viveiros, G. Angeles, S.R. Machado, A. Crivellaro, K.S. Rao, L. Junikka, N. Nikolaeva and P. Baas. 2016. IAWA list of microscopic bark features. *IAWA J.*, 37(4): 517-615.
- Bowes, B.G. 1997. *A colour atlas of plant structure*. Manson Publishing Ltd, UK.
- Dannoura, M., D. Epron, D. Desalme, C. Massonnet, S. Tsuji, C. Plain, P. Priault and D. Gérard. 2018. The impact of prolonged drought on phloem anatomy and phloem transport in young beech trees. *Tree. Physiol.*, 39(2): 201-210.
- den Outer, R.W. 1967. Histological investigations of the secondary phloem of gymnosperms. Thesis of Agricultural University, Wageningen, the Netherlands.
- Esau, K. 1969. *The Phloem. Encyclopedia of Plant Anatomy. Histology, Band. 5, Teil 2.* Gebrüder Borntraeger, Germany.
- Evert, R.F. 1990. Dicotyledons. In: (Eds.): Behnke, H.D. and R.D. Sjolund. *Sieve Elements. Comparative Structure, Induction and Development*. Springer, Germany, pp. 103-137.
- Evert, R.F. 2006 *Esau's plant anatomy: meristems, cells, and tissues of the plant body: their structure, functions, and development*. 3rd edition. John Wiley & Sons, Inc, USA.
- Franceschi, V.R., P. Krokene, T.K. Krekling and E. Christiansen. 2000. Phloem parenchyma cells are involved in local and distant defense responses to fungal inoculation or bark-beetle attack in Norway spruce (*Pinaceae*). *Amer. J. Bot.*, 87(3): 314-326.
- Gričar, J., P. Prislan, M. de Luis, K. Novak, L.A. Longares, E.M. del Castillo and K. Čufar. 2016. Lack of annual periodicity in cambial production of phloem in trees from Mediterranean area. *IAWA J.*, 37(2): 349-364.
- Gričar, J., S. Zavadlav, T. Jyske, M. Lavri, K. Eler and D. Vodnik. 2018. Effect of soil water availability on intra-annual xylem and phloem formation and non-structural carbohydrate pools in stem of *Quercus pubescens*. *Tree. Physiol.*, 39(2): 1-12.
- Hao, B.Z. and J.L. Wu. 1992. Ultrastructure of sieve elements in secondary phloem of *Dalbergia odorifera* during leaf-bearing and leaf-absent period. *Acta. Bot. Sin.*, 34(5): 360-363.
- Hesse, B.D., M. Goisser, H. Hartmann and T.E.E. Grams. 2018. Repeated summer drought delays sugar export from the leaf and impairs phloem transport in mature beech. *Tree. Physiol.*, 39(2): 192-200.
- Holbrook, N.M. and M. Knoblauch. 2018. *Physiology and metabolism: Phloem: a supracellular highway for the transport of sugars, signals, and pathogens*. *Curr. Opin. Plant. Biol.*, 43: III-VII.
- Holdheide, W. 1951. Anatomie mitteleuropäischer Gehölzrinden (mit mikrophotographischem Atlas). In: (Ed.): Freund, H. *Handbuch der Mikroskopie in der Technik*. Band 5, Heft I, Umschau Verlag, Frankfurt am Main, pp. 193-367.
- Hölttä, T., M. Mencuccini and E. Nikinmaa. 2009. Linking phloem function to structure: Analysis with a coupled xylem – phloem transport model. *J. Theor. Biol.*, 259(2): 325-337.
- Jyske, T. and H. Teemu. 2014. Comparison of phloem and xylem hydraulic architecture in *Picea abies* stems. *New. Phytol.*, 205(1): 102-115.

- Keeling, C.I. and J. Bohlmann. 2006. Genes, enzymes and chemicals of terpenoid diversity in the constitutive and induced defence of conifers against insects and pathogens. *New Phytol.*, 170(4): 657-675.
- Koh, E., L. Zhou and D.S. Williams. 2012. Callose deposition in the phloem plasmodesmata and inhibition of phloem transport in citrus leaves infected with "Candidatus *Liberibacter asiaticus*". *Protoplasma.*, 249(3): 687-697.
- Krekling, T., V.R. Franceschi, A.A. Berryman and E. Christiansen. 2000. The structure and development of polyphenolic parenchyma cells in Norway spruce (*Picea abies*) bark. *Flora.*, 195(5): 354-359.
- Li, Y. 2012. The changes of phloem structures and callose distributions during one year of growth in some conifers. Thesis of Nanjing Forestry University, Nanjing, China.
- Nedukha, O. 2016. Callose: Localization, functions, and synthesis in plant cells. *Cytol. Genet.*, 49(1): 49-57.
- Oparka, K.J. and T. Robert. 1999. Sieve elements and companion cells - traffic control centers of the phloem. *Plant. Cell.*, 11(4):739-750.
- Prislan, P., P. Mrak, Ž. Nada, Š. Jasna and M. Humar. 2018. Intra-annual dynamics of phloem formation and ultrastructural changes in sieve tubes in *Fagus sylvatica*. *Tree Physiol.*, 39(2): 262-274.
- Qie, G. and C. Wang. 2011. Spatial structure and health condition of street trees in Beijing built-up areas. *Urb. Environ. Urb. Ecol.*, 24: 9-12.
- Rockwell, F.E., J.T. Gersony and N.M. Holbrook. 2018. Where does Münch flow begin? Sucrose transport in the pre-phloem path. *Curr. Opin. Plant. Biol.*, 43: 101-107.
- Ronellenfitch, H., J. Liesche, K.H. Jensen, N.M. Holbrook, A. Schulz and E. Katifori. 2015. Scaling of phloem structure and optimality of photoassimilate transport in conifer needles. *P. Roy. Soc. B-Biol. Sci.*, 282: 20141863.
- Salmon, Y., L. Dietrich and D. Epron. 2019. Drought impacts on tree phloem: from cell-level responses to ecological significance. *Tree. Physiol.*, 39(2): 173-191.
- Schepper, V.D., T.D. Swaef, I. Bauweraerts and K. Steppe. 2013. Phloem transport: A review of mechanisms and controls. *J. Exp. Bot.*, 64(16): 4839-4850.
- Schulz, A. 1990. Conifers. In: (Eds.): Behnke, H.D. and R.D. Sjolund. *Sieve elements*. Springer, Germany, pp. 63-88.
- Sevanto, S. 2014. Phloem transport and drought. *J. Exp. Bot.*, 65(7): 1751-1759.
- Sevanto, S. 2019. Methods for assessing the role of phloem transport in plant stress responses. In: (Ed.): Johannes, L. *Phloem: Methods and Protocols, Methods in Molecular Biology*. Springer, Germany, pp. 311-336.
- Sjölund, R.D. 1997. The phloem sieve element: a river runs through it. *Plant. Cell.*, 9(7): 1137.
- Spicer, R. 2014. Symplasmic networks in secondary vascular tissues: parenchyma distribution and activity supporting long-distance transport. *J. Exp. Bot.*, 65(7): 1829-1848.
- Steppe, K., F. Sterck and A. Deslauriers. 2015. Diel growth dynamics in tree stems: linking anatomy and ecophysiology. *Trends. Plant. Sci.*, 20(6): 335-343.
- Suuronen, T.M.J.J. and A.V. Pranovich. 2015. Seasonal variation in formation, structure, and chemical properties of phloem in *Picea abies* as studied by novel microtechniques. *Planta*, 242(3): 613-629.
- Turgeon, R. and S. Wolf. 2009. Phloem transport: cellular pathways and molecular trafficking. *Annu. Rev. Plant. Biol.*, 60: 207-221.
- van Bel, A.J.E. 2003. The phloem, a miracle of ingenuity. *Plant. Cell. Environ.*, 26(1): 125-149.
- Wang, N. 2014. Comparative studies on secondary phloem in coniferous species. Thesis of Nanjing Forestry University, Nanjing, China.
- Yao, G., S. Wu, C. Hou, M. Zhang and D. Wang. 2012. Callose deposition at plasmodesmata is a critical factor in restricting the cell- to- cell movement of Soybean mosaic virus. *Plant. Cell. Rep.*, 31(5): 905-916.
- Zhao, G. and Z. Hu. 1985. Studies on the ultrastructure of secondary phloem in the stem of *Rhus verniciflua* stokes. *Acta. Bot. Bor.-Occ. Sin.*, 5: 77-82.

(Received for publication 4 June 2021)